Atmosfera (1997), **10,** *pp. 59-74*

Statistical structure of air surface temperature time series

OLEG O. RYBAK

Scientific Research Centre of the Russian Academy of Sciences, 8-a Theatralnaya Street, Sochi, 354000 Russia

(Manuscript received June 19, 1995; accepted in final form July 10, 1996)

RESUMEN

El cambio de la temperatura del aire en la superficie durante el último siglo es uno de los más controvertidos tópicos entre los investigadores preocupados con este problema. Sin embargo, la interrogante básica – si el aumento de la temperatura ha sido relacionado con las actividades humanas o ha sido el resultado de variabilidad climática natural – no ha sido resuelto aún. Sobresimplificación de procesos que contribuyen al sistema climático conducen a tomar en sentido erróneo la naturaleza del cambio climático. Se consideran los resultados del análisis de propiedades estadísticas de dos series de tiempo independientes. Se señalan cambios en la estructura estadística de la temperatura del aire en la superficie con el crecimiento de la escala de promedio espacial de local a global. Se discute la similitud entre el cambio de la temperatura global del aire y el camino al azar del beodo.

ABSTRACT

Surface air temperature changes during the last century is one of the most disputable topics among researchers concerned with the problem. Nevertheless, the basic question - whether the temperature growth has been connected with human activities or it has been the result of natural climatic variability - has not been solved yet. Oversimplification of processes driving the climate system leads to misundertanding the nature of climatic change. Results of analysis of statistical properties of two independent time series are considered. Changes in statistical structure of air surface temperature with the growth of the scale of spatial averaging from local to the global one are marked. Similarity between global air temperature changes and a random walk is discussed.

1. Introduction

The modern tendency in climatology may be briefly characterized as the revision of some stereotypes concerning global warming, its causes and consequences. This conclusion originates, at least, from the analysis of ". . . uncertainties in present theories of climate change and inadequate reliability of numerical modelling of anthropogenic climate changes, which formed the original basis of the greenhouse effect" (Kondratyev and Galindo, 1994). Increase of global surface air temperature since the year 1900 equals approximately to 0.5°C. This increase has been thought of to be connected mainly with human activities (rise of concentration of greenhouse gases). It is considered that the projected concentrations can produce future warming, and, as a result, lead to various economic and social problems. At the same time, our knowledge about the large-scale dynamic processes in the climate system of the Earth is far from being perfect. Now, most of the researchers agree, that major improvements should be brought in the conception of the climate system. As a result, the more careful judgements about the reasons of climate changes prevail: "The variability of trend estimates is sensitive to the structure of the temperature series on a time scale in the range of 50 to 500 years. Thus in order to evaluate the observed trend in the temperature series it is necessary to understand the natural variability of global temperature within this range" (Bloomfield and Nychka, 1992). Thorough statistical examination of a large amount of climatological record collected by today may enlighten the mechanisms of the internal climate variability and separate the changes caused by external forcing (human activities, volcanic eruptions, etc.) from those dependent on the temporal and spatial structure of the processes within the climate system.

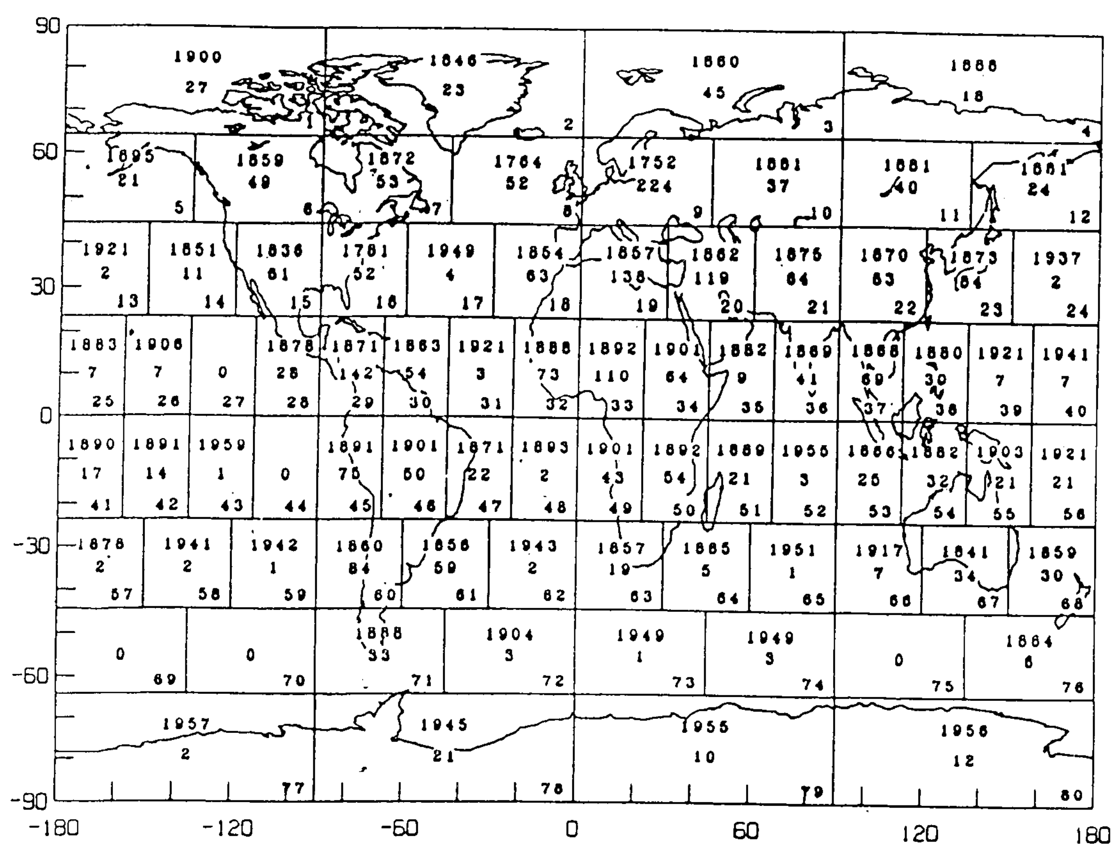

Fig. 1. Location of boxes with spatially averaged data. Total numer of stations in each of 80 regions of equal area, and when continuous coverage began for each region. A box identification number is given in the lower right-hand corner of the box (after HL87).

Climatologic records do not cover the surface of the Earth uniformly. Though methods of data spatial averaging vary from one climatic archive to another, a very useful information may be derived from the analysis of records which length equals or slightly exceeds a century. Below it will be demonstrated that the data obtained by different methods of spatial averaging have the similar internal statistical structure.

To get an objective picture of temperature changes we used two independent climatic data sets. Surface air temperature time series of different spatial averaging were taken from the papers by Hansen and Lebedeff (1987, 1988), mentioned below as HL. Series with the time step of one year cover the period of 1880-1987 (Fig. 1). Another one is TGMFL composed by World Data Centre (Obninsk, U. S. S. R.) by the end of 80th, covering the period of 1891-1986. In the current research the data are limited by 15°N in the South and by 80°N in the North. Methods of the data analysis are briefly observed in Section 2, results are collected in Section 3.

2. The method of analysis

Algorythms and computer program of autoregressive analysis used in the current research, were designed by Privalsky (1985). Below the procedure of computing is described briefly.

Autoregressive process x_t of the order p may be written as:

$$x_t = \phi_1 x_{t-1} + \ldots + \phi_p x_{t-p} + a_t, \tag{1}$$

where a_t is a sequence of independent identically distributed random values with zero mean and variance σ_a^2, ϕ_j - autoregression coefficients. The Burg algorithm (Ulrich and Bishop, 1975) is used to estimate parameters of autoregressive models (ARM) and Akaike criterion is used to choose the optimum AR order, $p = M$:

$$AIC(p) = \ln[(n-p)\hat{\sigma}_a^2] + 2p/n. \tag{2}$$

Here $\hat{\sigma}_a^2$ is the estimate of σ_a^2 and n is the length of a time series.

Time series may contain positive or negative linear trends. To make comparable with each other results of analyses of different time series, it is expedient to remove trends. For this purpose the procedure of extracting of a linear function (i.e., a trend) from the mixture of a linear function of time αt (α - the inclination angle) and white noise is suggested. Extracting is carried out by linear filtering with the weighting function (Roden, 1963):

$$h(n-1) = \frac{6}{n^2}\left(\frac{2t}{n} - 1\right), \quad t = 1, 2, \ldots, n. \tag{3}$$

Mean square error (MSE) of the estimate $\hat{\alpha}$ of the inclination angle α is defined as:

$$\hat{\sigma}_\alpha = \left(\frac{12\tilde{\sigma}_a^2}{n^3}\right)^{1/2} \tag{4}$$

Here $\tilde{\sigma}_a^2$ is the time series variance after removal of a trend. If $|\ \hat{\alpha}\ |$ exceeds $3\hat{\sigma}_\alpha$, a trend is considered to be statistically significant and is removed. To make distribution of trends more clear we compute statistically significant integral linear trends (i.e., inclination angles multiplied on lenght of respective time series) - ΔT.

Statistical predictability is characterized by the least-square relative prediction error (RPE) $d_p(\tau)$, where τ is the lead time. The lower RPE, the higher predictability. RPE (measured in percents) at the unit (that is one year) lead time $\tau - 1$, $d_p(1)$, is defined as:

$$d_\rho(1) = \sigma_a^2/\sigma_\xi^2 \times 100\% \tag{5}$$

where σ_ξ^2 - is the variance of a predicted process, σ_a^2 is the variance of white noise. The limit of statistical predictability τ_p, is defined as a limit lead time of a prediction, for which the NSE of a prediction remains lower than the variance of a predicted process (Monin, 1969). In accordance with the above definition, the limit of statistical predictability is achieved when RPE becomes no lower than some given value - the error level γ. The value $\gamma = 80\%$ was used as a limit level of predictability, though this value is quite arbitrary.

Spectral density function of autoregressive process of the order p is computed according to the Maximum Entropy Method (Ulrich and Bishop, 1975):

$$s(f) = \frac{2\sigma_a^2}{\mid 1 - \sum_{j=1}^{p} \phi_j e^{-i2\pi f} \mid^2}, \quad 0 \le f \le 0.5, \tag{6}$$

where f is frequency.

Table 1. Statistical paremeters of examined temperature time series.

Series	Integral linear trend ΔT, °C	Standard deviation $\hat{\sigma}_a$, °C	Standard deviation $\tilde{\sigma}_a$, °C	Optimum ARM order M	Relative prediction error, $d_1(p)$, %	Prediction limit $\tau(p)$, yr
HL:						
64.2-90°N	1.35	.7454	.6118	3	57.2	5
44.4-64.2°N	.72	.3725	.2964	5	87.4	1
23.6-44.4°N	.50	.2271	.1632	1	80.3	1
0-23.6°N	.44	.2210	.1738	3	86.0	1
0-23.6°S	.34	.2218	.1946	3	88.5	1
23.6-44.4°S	.32	.1662	.1327	1	83.8	1
44.4-64.2°S	.29	.2934	.2792	1	89.6	1
62.4-90°S	.69	.4752	.3993	0	-	-
NH	.61	.2617	.1772	4	71.1	2
SH	.39	.1761	.1761	1	89.6	1
Globe	.55	.2230	.1432	8	69.8	2
Box 6	.80	.7347	.6907	3	95.5	1
Box 7	.96	.6599	.5871	2	96.1	1
Box 15	.79	.4431	.3674	4	89.1	1
Box 16	.45	.3963	.3700	2	90.2	1
Box 9	-	.5633	-	3	95.2	1
Box 10	.94	.7037	.6402	0	-	1
TGMFL:						
65-80°N	.57	.5969	.5730	3	65.7	4
45-65°N	.26	.3103	.2994	4	89.0	1
25-45°N	-	.1895	-	2	61.3	3
15-25°N	-	.2134	-	1	76.2	2
15-80°N	-	.2018	-	2	63.6	3

The above mentioned statistical parameter - ΔT (integral linear trend), $\hat{\sigma}_a$ (standard deviation before removal of a trend), $\tilde{\sigma}_a$ (standard deviation after removal of a trend), M (the optimum order of ARM), $d_p(1)$ (RPE at the unit lead time) and τ_p (limit of statistical predictability), computed for all time series considered in the paper are collected at Table 1. Autoregressive models were fitted to original series after removal of statistically significant linear trends, so m, $d_p(1)$, τ_p and spectral densities were computed for stationary series.

Sample correlation function of the globally averaged air surface temperature (after HL) and its Maximum Entropy estimate are shown at Figure 2. Spectral densities of the HL temperature time series (zonal, hemispherical and global) are shown at Figs. 3 - 6. To compare statistical properties of the two data sets, HL and TGMFL, spectra of zonally averaged data are plotted at the same charts (Figs. 7 - 10).

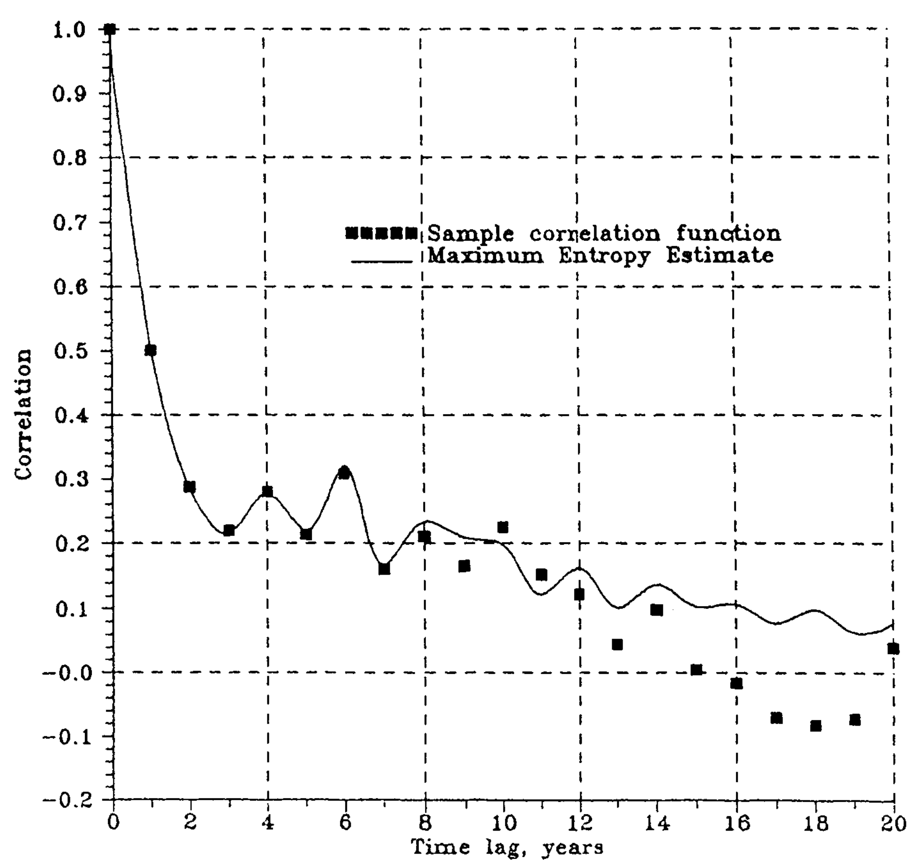

Fig. 2. Correlation function (sample and Maximum Entropy Estimate) of the global surface air temperature (after HL87).

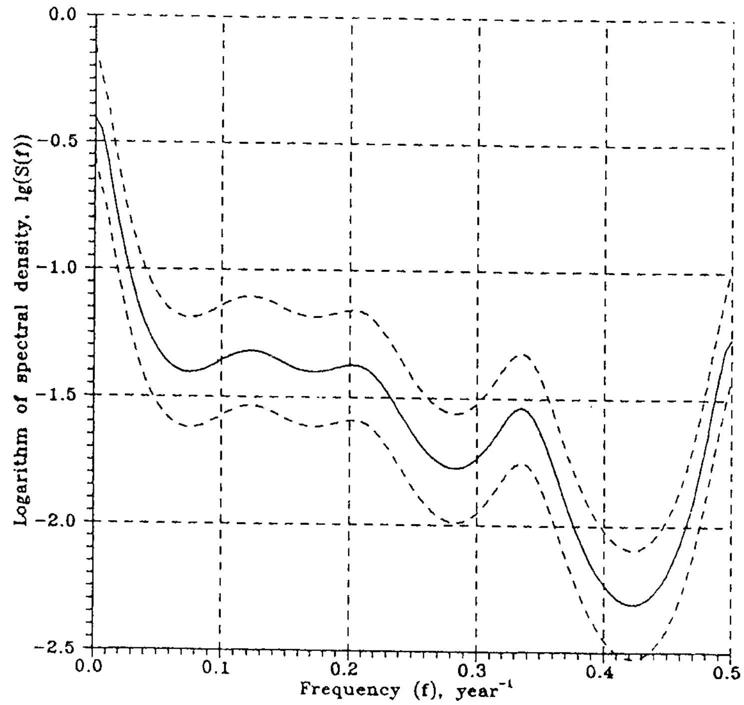

Fig. 3. Logarithm of spectral density of the global surface air temperature (after HL87) and its 90% confidence intervals.

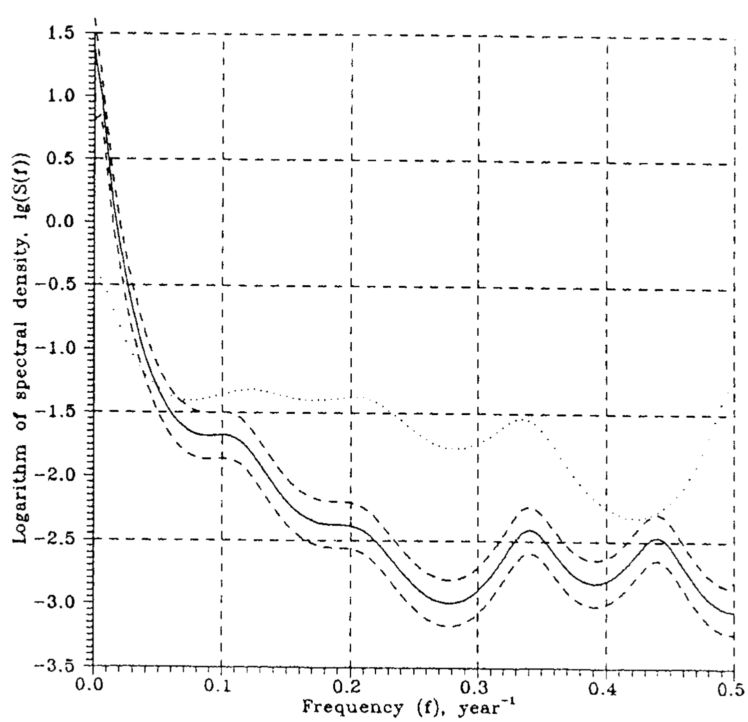

Fig. 4. Logarithms of spectral density of zonally and hemispherically averaged surface air temperature (after HL87) - Northern Hemisphere.

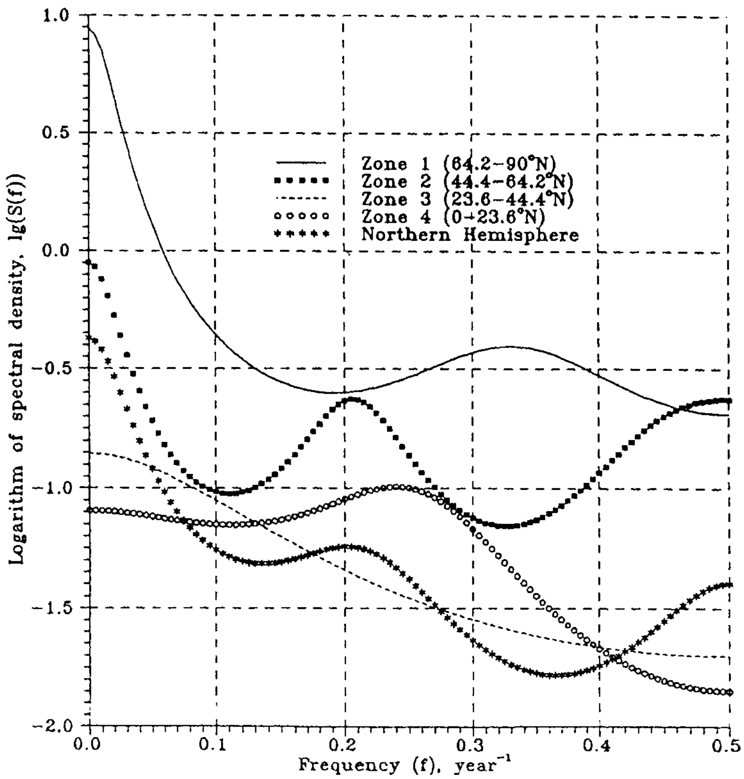

Fig. 5. Logarithms of spectral density of zonally and hemispherically averaged surface air temperature (after HL87) - Southern Hemisphere.

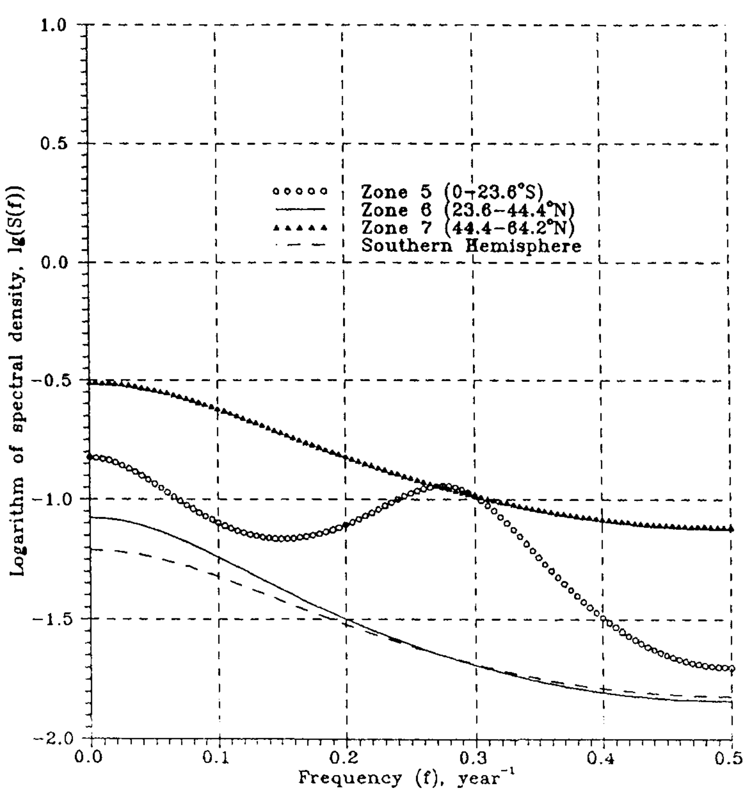

Fig. 6. Logarithms of spectral density of zonally averaged surface air temperature 64.2° - 90°N (after HL87) and 65° - 85°N (TGMFL) and their 90% confidence intervals.

3. Statistical characteristics

It is out of the scope of the paper to discuss the presence or absence of peaks in spectra of particular series and possible origin of the latter. In accordance with our point of view stated below, peaks in spectral curves may not mean that any particular physical reason is responsible for their presence. However, it should be noted that zonally averaged temperature series of the Northern Hemisphere and the data averaged over the hemisphere (excluding Zone 3: 23.6 - 44.4°N) are best approximated by ARMs different from the first order. At the same time, corresponding data of the Southern Hemisphere (excluding Zone 5: 0 - 23.6°S) is approximated by the ARM with $M = 1$, and the southernmost latitudinal strip series (Zone 8: 64.2 - 90°S) is approximated by white noise. We incline to explain this diversity by the lack of meteorological observations in the Southern Hemisphere, especially in Antarctic where the record is limited by 31 years in comparison with 108 years at other territories considered. It is notable that Zone 4 and Zone 5 adjacent to the equator have almost the same spectra ($M = 4$) with maxima which do not correspond to zero frequency. This "anomaly" - shift in spectral density maxima - being confirmed twice, points to distinction of thermal change processes in tropics with respect to the higher latitudes and the whole planet, being thought of to have "red spectrum" of temperature records.

The peculiar way of spatial averaging of HL data (Hansen and Lebedeff, 1987) seems to be responsible for the lower level of variance at all frequency in comparison with TGMFL (Figs. 6-10). However, the spectral functions computed for the same latitudinal strips are alike, especially in the middle and in the high latitudes. Incompletness of data in TGMFL which is limited by 15°N, is responsible, to our mind, for the distinctions in the hemispheric spectra.

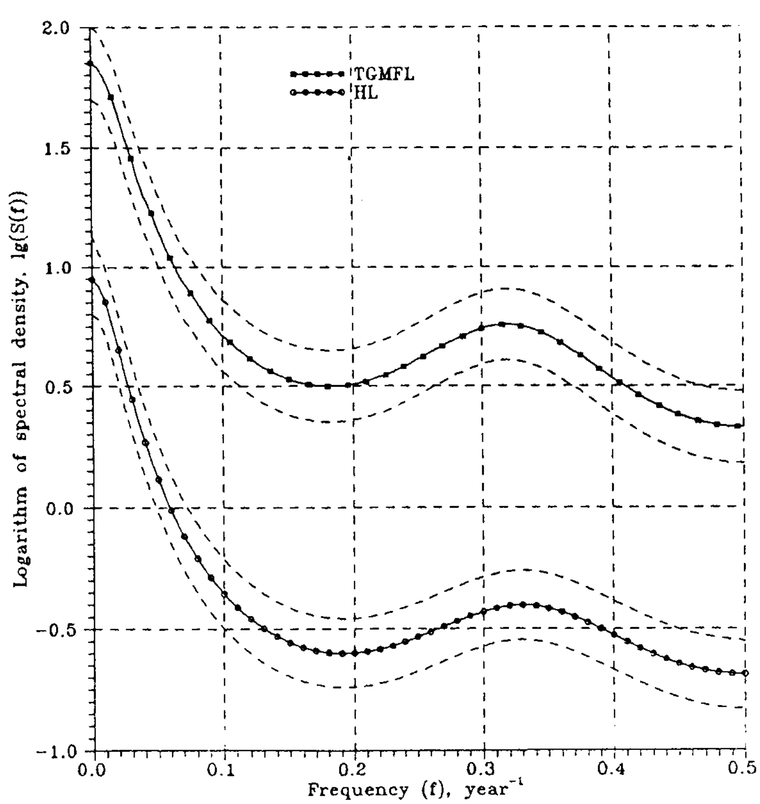

Fig. 7. Logarithms of spectral density of zonally averaged surface air temperatures 44.4° - 64.2°N (after HL87) and 45° - 65°N (TGMFL) and their 90% confidence intervals.

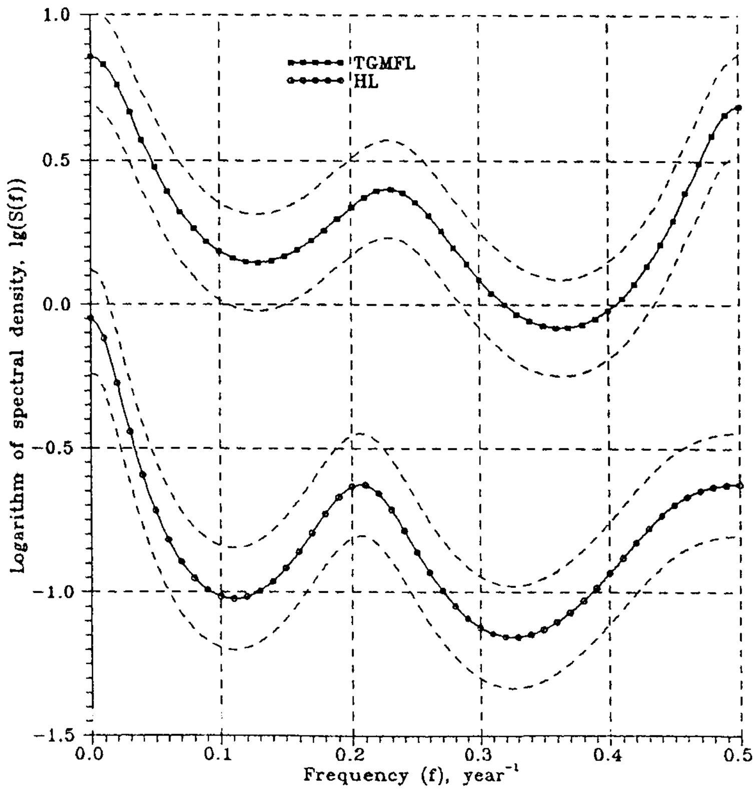

Fig. 8. Logarithms of spectral density of zonally averaged surface air temperatures: 23.6° - 44.4°N (after HL87) and 65° - 85°N (TGMFL) and their 90% confidence intervals

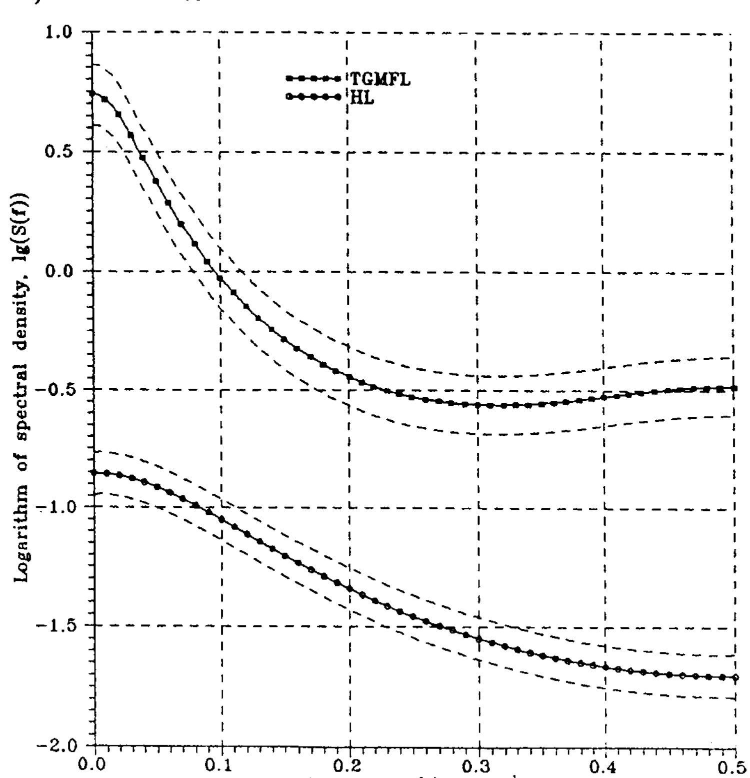

Fig. 9. Logarithms of spectral density of zonally averaged surface air temperatures: 0 - 23.6°N (after HL87) and 15° - 25°N (TGMFL) and their 90% confidence intervals.

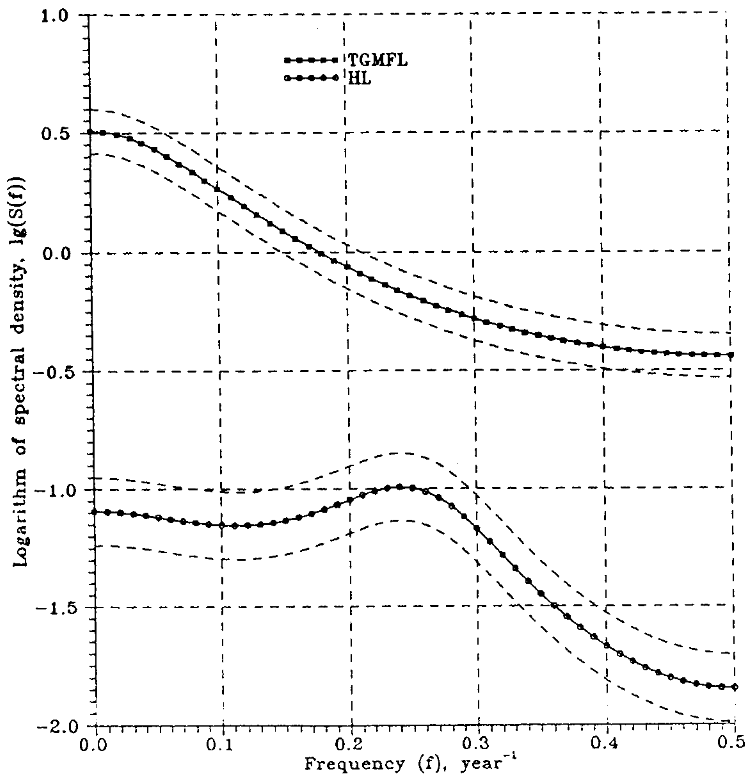

Fig. 10. Logarithms of spectral density of hemispherical averaged surface air temperatures: 0 - 90°N (after HL87) and 15° - 85°N (TGMFL) and their 90°confidence intervals.

HL zonally averaged data show distinct warming during the last century, rising of air temperature being more intensive in the high latitudes. Global warming values to 0.55°C. We failed to identify meaningful linear trends in TGMFL series in latitudinal belts south to 45°N and in the belt 15-80°N. Increase of temperature 45-65°N and at 65-80°N is somewhat lesser than computed for HL data set. The diversity in trend test results may partly be explained by the fact that TGMFL series are 12 years shorter than HL.

Increase of the spatial scale of averaging leads to the changes in statistical properties of the temperature time series.

Most of meteorological stations which have observed air surface temperature for a hundred or more years are located in Europe. Privalsky (1985) computed parameters of ARMs for several long climatic records and found that the optimum ARM order might vary from 0 to 6. The latter parameter was not dependent on duration of observations (from 138 to 315 years). All the records show low satistical predictability (high values of $d_p(1)$) $-$ $d_p(1)$ exceeded 95% in 13 cases of 20, and were lower than 90% only in 3 cases. This was true even for the longest record of the Central England, where $M = 4$ and $d_p(1) = 88\%$. The lowest $d_p(1) = 86\%$ was computed for the series of observations with the lenght of 164 years. It seems that neither the length of the series nor its ARM optimum order and, consequently the complicasy of the spectral density curve, has effect on the predictability of the air surface temperature at the local spatial scale. The limit of predictability (80% error level) has been overcome in a year.

No changes arise at the first step of averaging - over a territory of about 5,000,000 km^2. Almost all the meteorological stations mentioned above are located within the frontiers of the Box 9 (HL data set) covering European territory excluding Great Britain, Mediterranean Coast, Pyrenean Peninsula and the north of Scandinavia (224 meteorological station in total). Optimum ARM order $M = 3$, $d_p(1) = 95\%$. Zero is the optimum order for Box 10 (Western Siberia). The same results were obtained for the Boxes 6, 7, 15, 16 (Canada and the U. S. A., respectively (Table 1).

Air temperature of the whole latitudinal belt (Zone 2) is approximated by the ARM of the order 5, and $d_p(1)$ decreases to the value of 87%. Note that at Zone 1 (64.2 - 90°N) $d_p(1) = 57.2\%$ which is the lowest value in the data set, including the global temperature series. TGMFL shows higher values of predictability error.

Data averaged over the Hemisphere and the Globe show the decrease of $d_p(1)$ to 71% and 69.8% respectively. For TGMFL data averaged at the belt of 15-80°N the result is somewhat lower (63.6%). Privalsky (1985) gives the value of $d_p(1) = 53\%$ for the belts 15-90°N and 20-80°N but computed for TGMFL data set of the lenght of 86 years.

The global surface air temperature is approximated by the ARM with $M = 8$, its correlation function decreases quite slowly (Fig. 2). Not only the growth of M is important, but also the increase of statistical predictability with the growth of the averaging scale from local to hemispherical and global.

4. Climatic changes and a random walk

Dobrovolski (1992) stated the hypothesis that increase of the spatial scale of observational data averaging results in separation (polarization) of the autoregressive models of heat and water exchange processes in the climate system of the Earth. Those parameters connected with matter of energy accumulation in any natural reservoir, tend to the Wiener process (random walk) with the growth of spatial averaging. Air temperature, ocean surface temperature World Ocean level, are thought of to be such parameters. Those ones which characterize the intensity of matter or energy exchange (evaporation, moisture transport, precipitation, river run off) tend to a white noise with transition from local scale to the global ones.

From the point of view of physics this phenomenon may be explained by weakening the feedbacks while transiting from local scales to the global one. It is natural that the growth of the spatial scale l entails ($\sim l^2$ or $\sim l^3$) increase in heat and moisture capacity of reservoirs involved in heat and moisture circulation. At the same time, the intensification of anomalous heat and moisture fluxes between these reservoirs occurs much slower due to a limited radius of the spatial correlation between these fluxes (Dobrovolski, 1992; Dobrovolski and Rybak, 1994).

The hypothesis of Dobrovolski agrees with the hypothesis of Hasselmann (1976) which states the separation of scales of processes in the climatic system. Indeed, in accordance with Hasselmann, there are, at least, two groups of processes to be considered in the climatic system (generally speaking, the entire hierarchy of such processes exists). These groups are characterized by the reply time for the external forcing. Hasselmann calls these procceses "weather" and "climatic" variables. Rapidly changing "weather" variables influencing the inertial, slowly changing parts of the climate system ("climatic" variables) cause the gradual evolution of the latter. In turn, the changes in state of "climatic" variables determine new frontiers limiting the behaviour of the "weahter" variables. In other words, changes of the inertial components of the climate system set new boundary conditions for "weather variables. In such a manner the feedback between the processes of different scales is maintained. In accordance with the hypothesis, the generalized spectral density of the "climatic" variables is approximated by the "red" noise - with a gradual decrease of oscillation energy with increase of frequency.

Numerical experiments with models of ocean surface temperature constructed on the basis of Hasselmann hypothesis (Hasselmann and Frankignoul, 1977; Dobrovolski, 1982; Rybak, 1992) demonstrated that large-scale anomalies of "climatic" variables are of local origin, in a great extent.

The growth of the spatial scale of matter and energy exchange processes inside the climate system results in weakening of feedbacks. It happens because of the finite correlation of the radius of the "weather" variables, which in turn is dependent on the dimension of synoptical scales (Dobrovolski, 1992). As it was demonstrated in Section 3, certain changes occur in the statistical features of the climatic series while spatial averaging increases. Gordon (1991) stated the idea of the resemblance between the changes of the global surface air temperature and a random walk. From the point of view of Gordon, the climate system is subjected to positive and negative random shocks, which are accumulated by the system, and, at last, result in a random walk-like evolution of air temperature, for example, Gordon did not stress at the physical origin of "shocks", but it was obvious that they could be either of natural (internal or external) or artificial (pollution with greenhouse or ozone destructing gases).

The above statements of Gordon and Dobrovolski have an extention. The Wiener process is the limit case of a random walk, when its step is infinitely small. It may be considered also as a limit case of a fractional noise. The latter in general case may be expressed as a linear ARM of the infinite order (Andel, 1986).

In accordance with Dobrovolski (1992), the variability of the global air temperature climatic time series approaches to the Wiener process. Hence, one could expect arising of difficulties of its approximation by ARMs. Indeed, the optimum order of the respective ARM equals to 8. The optimum order growth may point to the fact that a model of fractional order might be the better approximation to the global processes. Fractional noises have infinite time of correlation ("long memory"). In case such a model were best fitted to a time series, we could speak about existence of time teleconnections in a series. Rather long positive correlation of the global air surface temperature (Fig. 2) illustrates the above statements.

It would be reasonable to suppose that transition of moisture and heat exchange processes from local scales (comparable with the character dimension of a cyclone) causes changes in statistical structure of processes themselves. In the statistical sense, the variability of the local processes confirms to the Hasselmann hypothesis, the variability of the global ones is close to a random walk or to its general case - a fractional noise process.

This statement may be illustrated by the numerical experiments (Privalsky *et al.*, 1992) aimed at constructing the models of fractional orders of TGMFL zonally averaged data and comparing results obtained with fitting of the usual (linear) ARMs. Series of the ARM orders 1 - 3 (following Akaike criterion) were better approximated by fractional noise models. And those series which optimum orders varied from 4 to 7 were better fitted by linear ARMs. It may be concluded that zonally averaged series (of the intermediate spatial scale - between local and global) which have, in general, the uniform statistical structure, are fitted either by linear ARMs of the rather high orders or by the simpler fractional order models.

Gordon (1991) speculated that in the climatic system which behaviour resembled one-dimensional random walk, statistically significant positive and negative trends might rise. Feller (1960) pointed that this property was general for the systems "accumulating" positive and negative steps, independently of their origin. At the first glance, this feature which is peculiar to the wide class of the natural phenomena may be thought of to have no physical explanation. It means that we deal with one of the most fundamental laws of Nature connecting random and deterministic phenomena.

A simple numerical experiment may give an idea of how changes in the climatic system might be perceived by an external observer. Let us generate pseudorandom values with Gassian distribution, zero mean and standard deviation taken from observations. In our case standard deviation equals to 0.1432°C (Table 1). Pseudorandom values are to be summed cumulatively in order to obtain a new series of partial sums. After these operations we get a model of a realization of the one-dimensional random walk.

Table 2. Statistical paremeters of simulated temperature time series.

Simulated series and their lengths, yr	Integral linear trend ΔT, °C	Standard deviation $\hat{\sigma}_a$, °C	Standard deviation $\tilde{\sigma}_a$, °C	Optimum ARM order M	Relative prediction error, $d_1(p)$, %	Prediction limit $\tau(p)$, yr
50	1.43	.4955	.1041	8	15.4	8
100	2.80	.8973	.1622	2	7.7	12
200	2.88	1.0309	.5531	10	2.0	33
300	3.79	1.2454	.5327	1	2.4	65
500	5.37	1.7428	.5416	2	2.9	47
1000	4.84	2.0738	1.5207	1	0.9	> 100
5000	2.24	2.0884	1.9868	1	0.5	> 100

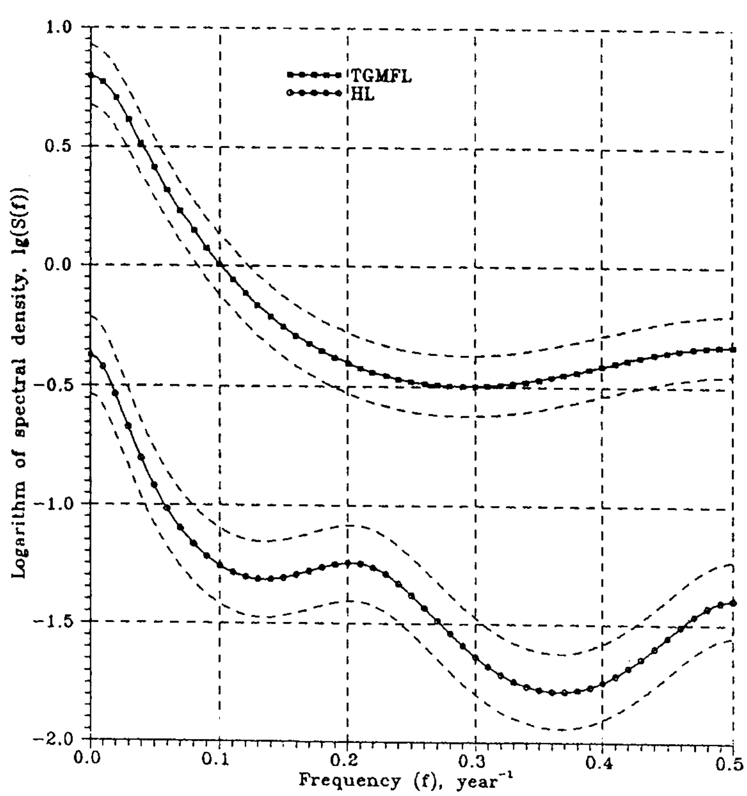

Fig. 11. Logarithm of spectral density of the global surface air temperature (simulated series) and its 90% confidence intervals. Spectrum of measured one is shown by the dashed line.

Satististical features of the simulated series of different lengths are collected at Table 2. Corresponding spectral density functions are plotted at Figs. 10 and 11. All series figure genuine linear trends. Thus, our speculations about the possibility of appearing of spontaneous increase or decrease of air temperature, for example, are supported by simple experiment based on conception stating random, to a great extent, nature of the climate evolution.

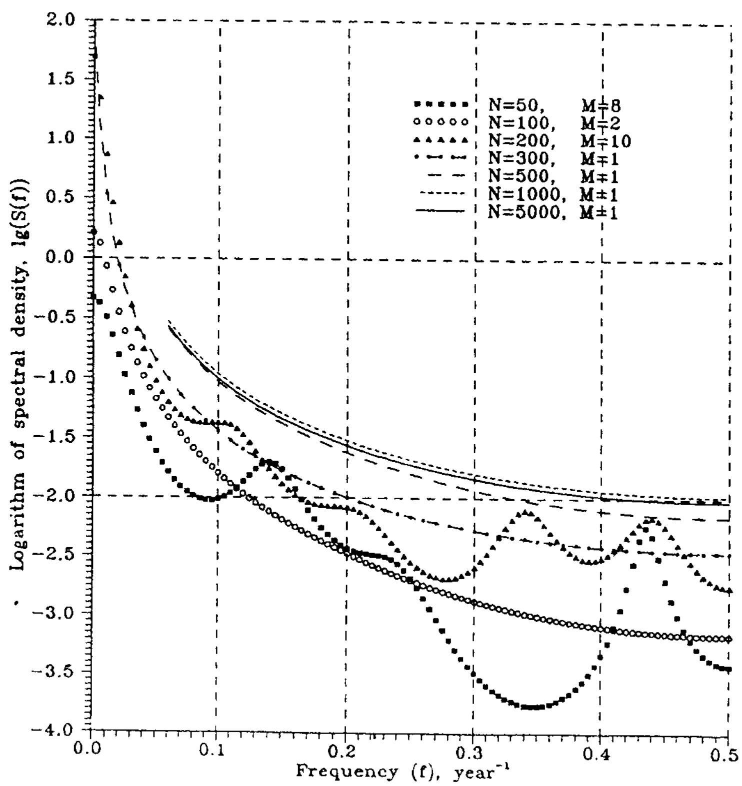

Fig. 12. Logarithms of spectral density of simulated series of different lengths.

It is interesting that optimum ARM orders (M) of simulated series change with the growth of series' lenght (N). ($M = 8$ for $N = 50$, $M = 2$, for $N = 100$, $M = 10$ for $N = 200$, $M = 1$ for $N = 300$ and more). In any case, when $M > 2$, statistically significant peaks may arise in high frequency domain of spectra. Beginning with $N = 300$ M does not exceeds 1, and spectral function becomes proportional to f^{-2}. Statistical features of a simulated series may vary dependently not only on length of a series but also from one particular parcel of examined series to another. Statistical predictability of a simulated series exceeds the corresponding characteristic of the observed records. Thus, a random walk serves as an idealization of the really existing exchange processes.

5. Summary

The objective analysis of historical time series evidence that the climate of the Earth undergoes the period of coolings and warmings of different durations. Long-period temperature fluctuations are considerably ununiform in space. Regions of temperature (both air surface and ocean surface) increase coexist with regions of cooling. Non-uniform character of trend distribution may be the consequence of the local, in general thermal anomalies origin.

Analysis of air temperature records makes us think that regional climate subsystems loose in feedback intensity while growth of spatial scale of the latter. This phenomenon is responsible for changes in spectral properties of the "climatic" (following Hasselmann's definition) variables - predominating of ARMs of order higher than the first, growth of statistical predictability.

Weakening of feedbacks in the processes of the global scale leads to converting of temperature changes into the Wiener process. Long durations of positive and negative values inherent to random walks may be identified as a deterministic process of temperature growth due, for example, to human activities. Such a possibility does not mean that man cannot influence on the heat exchange processes in the climate system. On the contrary, existence of natural trends may hide the negative influence for some time, and afterwards lead to unpredictable catastrophic results which may occur quite unexpectedly and in an "explosion" manner due to nonlinearities of natural system.

Though our arguments are rather speculative they are capable to enlighten the very difficult and important problem of the nature of the Earth's climate.

Acknowledgements

This work has been supported by the International Association for the Promotion of Cooperation with Scientists from the Independent States of the Former Soviet Union - Project INTAS 93-0979 "Global Ice Sheets During the Last Two Climatic Cycles, with the Emphasis on Entering into New Glaciation". Author expresses his gratitude to Dr. Privalsky who provided with the data set of the global surface air temperature (TGMFL) and computer programs for processing the time series.

REFERENCES

Andel, J., 1986. Long Memory Time Series Models. *Kybernetica,* **22**, 105-123.

Bloomfield, P. and D. Nychka, 1992. Climate spectra and detecting climate change. *Clim. Change.*, **21**, 275-287.

Dobrovolski, S. G., 1982. Simple dynamic-stochastic model of the large ocean surface temprature anomalies. *Meteorologija i gidrologija*, **6**, 68-75 (in Russian).

Dobrovolski, S. G., 1992. Global Climatic changes in Water and Heat Transfer-Accumulation Processes. *Elsevier*, Amsterdam. 280 pp.

Dobrovolski, S. G. and O. O. Rybak, 1994. On the Phenomenon of Local-Global Polarization. In: *Contemporary Climatology* (Ed. by R. Brazdil), Brno, 165-168.

Feller, W., 1960. An Introduction to Probability Theory and its Applications. Vol. 2, *John Wiley*, New York.

Gordon, W., 1991. Global Warming as a Manifestation of a Random Walk. *J. Clim.,* **4**, 589-197.

Hansen, J. and S. Lebedeff, 1987. Global Trends of Measured Air Surface Temperature, *J. Geophys. Res.*, **92**, 13345-13372.

Hansen, J. and S. Lebedeff, 1988. Global Surface Air Temperatures: Update through 1987. *Geophys. Res. Lett.*, **15**, 323-326.

Hasselmann, K., 1976. Stochastic climate models. Part 1 Theory. *Tellus*, **28**, 473-485

Hasselmann, K. and C. Frankignoul, 1977. Stochastic climate models. Part 2. Application to sea-surface temperature anomalies and thermocline variability, *Tellus*, **29**, 289-305.

Kondratyev, K. Ya. and I. Galindo, 1994. Global climate change in the context of global ecodynamics, *Geofís. Int.*, **33**, 487-496.

Monin, A. S., 1969. Weather prediction as a task of physics. *Nauka Publishers,* Moscow, 184 p. (in Russian).

Privalsky, V. E., 1985. Climatic variability. Stochastic models, variability, spectra. *Nauka Publishers*, Moscow, 184 p. (in Russian).

Privalsky, V. E., V. A. Panchenko and E. Y. Asarina, 1992. Time Series Models with Applications to Geosciences, *Gidrometeoisdat*, Saint-Petersburg, 226 p. (in Russian).

Roden, G., 1963. Sea level variations in Panama, *J. Geophys. Res.*, **68**, 5701-5710.

Rybak, O. O., 1992. On the application of a dynamic-stochastic climate model to the simulation of the oceanic upper layer thermal variability. *Atmósfera*, **5**, 181-192.

Ulrich, T. and T. Bishop, 1975. Maximum entropy spectral analysis and autoregressive decomposition, *Rev. Geophys. Space Phys.*, **13**, 183-200.